Pneumatic Tyre Aquaplaning: an Experimental Investigation on Manifestations and Influences of Appearance

Andreas Fichtinger[1], Ádám Bárdos[2], Zsolt Szalay[2], Johannes Edelmann[1], Manfred Plöchl[1]

[1] Institute of Mechanics and Mechatronics, TU Wien, Getreidemarkt 9, 1060 Vienna, Austria, e-mail: andreas.fichtinger@tuwien.ac.at, johannes.edelmann@tuwien.ac.at, manfred.ploechl@tuwien.ac.at

[2] Department of Automotive Technologies, Budapest University of Technology and Economics, Stoczek utca 6, 1111 Budapest, Hungary, e-mail: bardos.adam@kjk.bme.hu, szalay.zsolt@kjk.bme.hu

Abstract: Aquaplaning at wet road conditions and high speeds can be a source of dangerous driving situations and accidents. The proper understanding of characteristic effects can be crucial in early aquaplaning detection and accident avoidance, essential for driver and driver assistance systems and trajectory planning for self-driving cars. Four test vehicles were equipped with a basic measurement system, and measurements were performed to evaluate characteristics of aquaplaning, such as wheel spin-up and wheel spin-down, change of rolling resistance, tyre slip slope, and tie rod force. Driveline configuration, type, wear and inflation pressure of the tyre(s), water level height next to chosen speed and performed manoeuvre significantly affect vehicle behaviour and thus the possibility to detect aquaplaning conditions. The results and main findings may allow and help establish corresponding methods to early detect aquaplaning and dangerous driving conditions.

Keywords: Aquaplaning; Hydroplaning; Vehicle Dynamics; Advanced Driver Assistance Systems, Active Safety Systems; Identification and Estimation

1 Introduction

Rain and wet road conditions frequently cause critical driving situations and may result in accidents. While damp roads with thin water level heights are the cause of only a minor reduction of the maximum tyre forces, larger water level heights at higher speeds may lead to aquaplaning. The latter situation may become critical when aquaplaning appears suddenly and unexpectedly, and the longitudinal and lateral friction coefficients will drop to a level close to zero. Loss of vehicle control

and, in the worst case, loss of stability may be the consequence. Wet road conditions contribute considerably to road accidents, [1]. [2] indicates that approximately 20% of accidents occur at wet road conditions. However, the evaluation of the exact share of aquaplaning is difficult, [3], [4]. Also, questions on liability at aquaplaning related accidents are challenging [5], in particular referring to influences from tyre conditions, road maintenance, and vehicle speed.

This paper addresses a comprehensive experimental investigation on pneumatic tyre aquaplaning considering a variety of realistic driving and environmental conditions. Characteristic effects that may indicate the appearance and intensity of aquaplaning, such as wheel spin-up and wheel spin-down, change of rolling resistance, tyre slip slope, and tie rod force, will be analysed in more detail. None of these effects is unique to aquaplaning, but can also be observed for other tyre–road conditions, as for snow covered roads, to give just an example. In addition, and in particular studied here, several other actual facts show a strong influence, these include: vehicle speed and performed manoeuvre, water level height, type, wear and inflation pressure of the tyre(s), and last but not least, the driveline concept, i.e. front-wheel (FWD), rear-wheel (RWD) and all-wheel drive (AWD). The revealed findings may promote the development of an on-board algorithm that combines presented characteristic effects and may allow to detect early aquaplaning, and therefore prevent serious driving situations such as loss of stability.

The extensive investigation of pneumatic tyre hydroplaning has started as early as in the 1950s by NASA, mainly with the aim to prevent hydroplaning of aircraft tyres on wet runways. At the hydroplaning speed the hydrodynamic lift developed under the tyre equals the partial weight of the vehicle acting on the tyre and any further increase in speed beyond this critical speed must force the tyre to lift completely off the runway surface, which is termed total aquaplaning, from [6]. Subsequently, the tyre is defined to be partially/total aquaplaning at speeds below/above the aquaplaning speed. As the hydrodynamic pressure is a function of vehicle speed, and by ignoring tread design and surface texture and assuming the fluid depth on the surface to be greater than tyre tread groove depths, a simple relation for the hydroplaning speed V_p is giving in [6],

$$V_p = k_1 \sqrt{\frac{F_V}{A_G}} \sim k_2 \sqrt{p} \quad , \tag{1}$$

with parameters $k_1, k_2,$ vertical tyre load F_V, gross tyre contact area $A_G,$ and inflation pressure p of the tyre. Already this simple formula reveals key influences that will be considered in the following chapters. A similar empirical formula for automobile tyres is given in [7], which incorporates the water level height as well.

At speeds below the hydroplaning speed, the contact area may be considered to comprise three zones, which is illustrated in Figure 1 [8]. In zone A, the tyre contacts the water film and the bulk of the surface water is displaced away from the path of the tyre or into the grooves. Zone B is a transition, a thin-film zone, where partial hydroplaning occurs. In zone C, the water film has been totally or

substantially removed, the tread rubber and road surface are in intimate dry contact and dry road friction conditions prevail, [8].

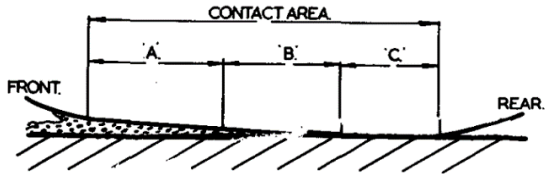

Figure 1
Illustration of three zone contact area modelling [8]

The dimensions of the individual zones will typically not be constant when driving on a wet road with varying conditions and speeds. With increasing speed, the bulk zone penetrates towards the rear edge of the contact area. While the dry road contact section is narrowing, the effective friction coefficient of the tyre decreases progressively. Finally, at total hydroplaning, the bulk zone fully dominates the "contact area" and the effective coefficient of friction is substantially zero. Hence, the control of vehicle dynamics by the tyres forces cease. The progression of aquaplaning with increasing speed is graphically portrayed in Figure 2, confirming the findings presented in [6]. A comprehensive study about the contact patch deformation and tyre carcass deflections during aquaplaning is published in [9] and [10], utilizing accelerometers and optical sensors installed at the inner layer of the tyre.

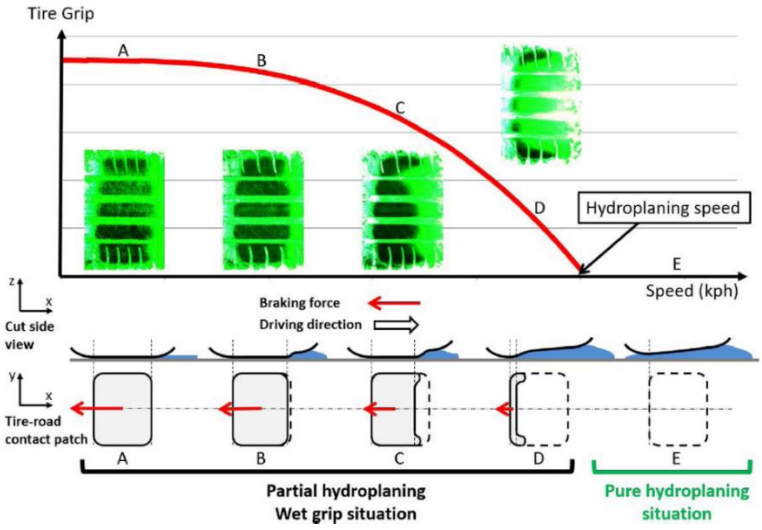

Figure 2
Diminishing of tyre grip during the evolution of aquaplaning [3]

Many different characteristic effects of hydroplaning were examined in relation to investigations of aircraft tyres. Aquaplaning behaviour of free rolling aircraft wheels, represented as a single wheel in combination with a bogie, is presented in [11], where wheel spin-down and various influences thereon are described. [12] focuses on the influence of tyre inflation pressure, tread depth, and tread width, together with the macro texture of the pavement on the wheel spin-down effect. [13] lists eight types of characteristic effects of hydroplaning and presents measurement results with specifically instrumented tyres and wheel fixtures on different runways. Hydrodynamic pressure measurements and glass plate photographs provide essential information for the understanding of the tyre-ground contact shape and the pressure variations. [14] investigates wheel spin-down besides tyre parameters. Very comprehensive observations of the hydroplaning effects are given in [6]. In this study, eight characteristic effects are analysed: the detachment of the tyre footprint, the hydrodynamic ground pressure variation, the wheel spin-down, the suppression of tyre bow wave, the scouring action of escaping fluid, the peaking of the fluid displacement drag, the loss in braking traction, and the loss of directional stability. [15] gives an overview of the hydroplaning phenomenon.

In addition to the above investigations, other aquaplaning effects can be sensed, in particular on vehicle level, and are also of practical relevance. For example, the driver can usually feel aquaplaning as a decrease in steering wheel torque and responsiveness to steering input, and for cars with front-wheel drive, as an increase of engine speed during acceleration. Irregular water films under the right and left wheels may cause permanent or a series of short pulse drags at the individual wheels owing the increased rolling resistance at varying aquaplaning conditions.

The paper is organized as follows: Chapter 2 briefly introduces the applied measurement setup. Chapter 3 analyses the measured individual characteristic effects of aquaplaning, organized into five sub-chapters to address wheel spin-down, wheel spin-up, rolling resistance, tyre slip slope, and steering tie rod force change, respectively. Influences of different driveline configurations (FWD, RWD, and AWD), tyre types (including summer and winter tyres), inflation pressures, and water level heights will be discussed for different driving manoeuvres and vehicle speeds. In Chapter 4, main conclusions are drawn and possible utilization of the findings briefly addressed.

2 Measurement Setup

Four different vehicles were used to represent different driveline configurations, one front-wheel (FWD), two rear-wheel (RWD), and one all-wheel drive (AWD) vehicle. All of the cars were equipped with a dual antenna differential GNSS system to monitor the vehicle's motion accurately. With direct access to the vehicle data BUS communication provided by an Inventure Automotive FMS Gateway, the

following signals were recorded during each of the test runs: individual wheel speeds, actual engine torque and speed, current gear, driveline engagement, steering wheel position, accelerator pedal position, brake pressure, and 3-axis accelerations/angular velocities from an inertial measurement unit (IMU). At the AWD vehicle also the tie rod forces were measured. The actual water level heights were continuously recorded by an optical Lufft MARWIS sensor [16], see corner of Figure 3.

For the FWD vehicle tests (vehicle A), a front-engine car was used, equipped with one year old medium worn summer tyres of dimension 205/55 R16V (~ 5 mm tread depth), Figure 3. The nominal tyre inflation pressure was 2.3 bar at the front tyres and 2 bar in the rear tyres. The mass of the vehicle was about 1450 kg during the tests.

For the RWD vehicle tests a rear-engine (vehicle B) and a front-engine (vehicle C) car were used. Vehicle B was equipped with three years old (very) worn summer tyres of dimension 245/35R20 at the front axle (~5 mm tread depth) and dimension 305/30R21 at the rear axle (~2 mm tread depth). The lowest recommended and called here the low or nominal tyre inflation pressure, was 2.2 bar at the front tyres and 2.3 bar at the rear tyres. The actual mass of the vehicle was about 1750 kg during the tests. Vehicle C was equipped with almost new slightly worn summer tyres of dimension 245/35R19 at the front axle (~7 mm tread depth) and dimension 265/35R19 at the rear axle (~ 7 mm tread depth). The nominal tyre inflation pressure was 3 bar at all tyres. The mass of the vehicle was about 1800 kg during the tests.

For the AWD vehicle tests, a rear-engine vehicle was used. Vehicle D was equipped with three years old medium worn summer tyres of dimension 245/35R20 at the front axle (~ 4.5 mm tread depth) and dimension 305/30R20 at the rear axle (~ 4.5 mm tread depth). The nominal tyre inflation pressure was 2.4 bar at the front tyres and 2.7 bar in the rear tyres. The actual mass of the vehicle was about 1910 kg during the tests.

Figure 3
FWD Vehicle A on wet lane, watered with sprinklers; MARWIS sensor, [16], to measure water level heights

The measurements were carried out on two separate lanes of the ZalaZONE Automotive Proving Ground [17] braking platform. For tests performed with deeper (more than 2 mm) water levels an aquaplaning basin was used, where a calm and

constant water level height can be adjusted. For water level heights less than 2 mm, an asphalt lane without lateral grade was chosen with adjustable water sprinklers on the lane's left-hand side, see Figure 3, to set a defined water level height from 0.6-2 mm.

3 Experimental Study of Different Characteristic Effects of Pneumatic Tyre Aquaplaning

3.1. Wheel Spin-Down

Probably the most easily observable characteristic effect of partial or total aquaplaning is the slowdown of free-rolling (undriven and unbraked) vehicle wheels and corresponding drop of rotational wheel speeds. The wheel-spin down effect can be explained on a physical basis. With increasing vehicle speed, a growing water wedge develops progressively at the front area of the tyre ground contact area, see Figure 2 (tyre footprints A to E), back to the rear, reducing the size of the dry zone, where the tyre adheres to the ground (zone C in Figure 1). Finally, the tyre footprint will disappear, which marks the aquaplaning speed resulting in total tyre aquaplaning. Then, the vertical force developed by the water hydrodynamic pressure is in balance with the vertical tyre load. At (partial) aquaplaning, the centre of the hydrodynamic lifting force is located forward of the wheel centre which causes a moment opposing the drag forces on the tyre; as this moment increases, the spin-down of the wheel begins, [18].

Measurement results for RWD vehicle C clearly reveal the wheel-spin down effect of the free-rolling front wheels as shown in Figure 4(a). The output rate of the water sprinkler was set to provide a constant water level height of 1.1 mm. The speed of the test runs was incremented by 10 km/h steps from 70 km/h to 110 km/h to cover the relevant region of possible aquaplaning for the medium worn summer tyre. After accelerating to the target speed on a flat dry road, the wet area was entered at 10 s. Then, the driver holds the target speed, usually by a moderate increase of the accelerator pedal position due to the increased rolling resistance on the watered area. At the end of the watered lane the vehicle was stopped.

At 70 km/h target speed, there appears no sign of partial aquaplaning from wheel spin-down, the speeds of front wheels coincide with the measured GPS velocity v_x of the vehicle. At 80 km/h target speed, the first very minor signs of the spin-down events appear at the front right wheel from the hardly noticeable mismatch with the vehicle velocity. With increasing speed, continuous and minor as well as individual and pronounced spin-down events, show up. Roughly speaking, total aquaplaning at the front right tyre could be attributed close to 100 km/h.

Corresponding to Figure 4(a), the longitudinal slip s_x for the front tyres are derived and plotted as function of target speed in Figure 4(b). The required effective rolling radius has been adopted from the dry asphalt lane. It turns out that the longitudinal slip of the front right tyre decreases with speed in an exponential manner for these constant speed manoeuvres. The front left tyre shows only minor slip events. The reason is that the water sprinklers are located on left-hand side in driving direction with slightly more water on the right-hand side of the lane and therefore reducing aquaplaning speed.

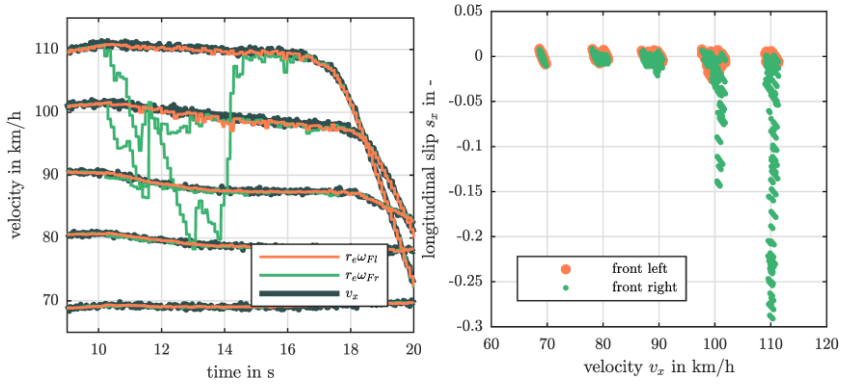

Figure 4

(a) Wheel spin-down events at the front non-driven wheels of RWD vehicle C;

(b) Longitudinal slip of the front tyres of RWD vehicle C corresponding to (a);

1.1 mm water level height; medium worn summer tyres; nominal inflation pressure

Figure 5(a) shows all wheel speeds of FWD vehicle A for the constant speed test runs. The watered lane starts again at 10 seconds. No total aquaplaning appears at any tyre, and first signs of partial aquaplaning with continuous light spin-down events of the rear right wheel turn up at 105 km/h target speed. The extent of spin-downs of the FWD vehicle is much smaller compared to the RWD vehicles for two main reasons: first, at the FWD vehicle, the rear wheels are free-rolling in the cleared path of the front wheels with a smaller height of the remaining water film. Secondly, tyre type, size, and load is different for the two test vehicles. At the driven front wheels, continuous slight spin-ups appear at higher speeds.

After increasing the water level height from 0.8 mm to 1.8 mm, Figure 5(b), spin-down events at the rear right wheel show up more clearly. At the same time, 10-14 s, obvious and pronounced spin-up events at the front right wheel indicate that although the driver intends to balance the increased rolling resistance and to keep the vehicle speed constant by pushing the accelerator pedal, the vehicle slightly slows down in this period from loss of traction.

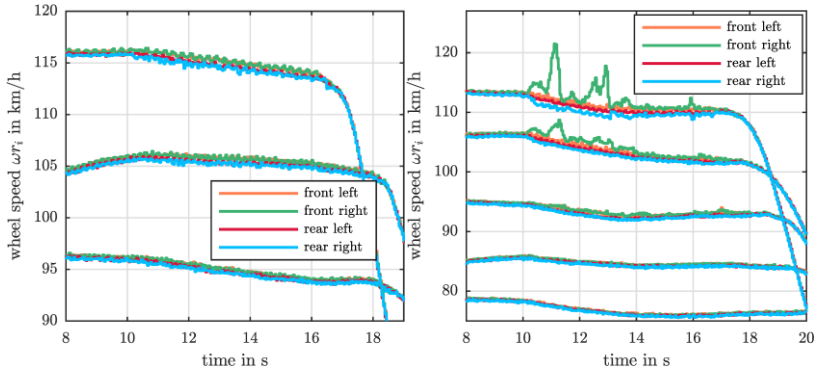

Figure 5
Wheel spin-down and spin-up events at FWD vehicle A; (a) 0.8 mm water level height; (b) 1.8 mm water level height; medium worn summer tyres; nominal inflation pressure

3.2. Wheel Spin-Up

Drivers usually do not sense spin-down events of the free-rolling wheels on wet surfaces, but often detect the loss of traction from the sudden increase of the engine speed, especially when accelerating, due to partial or total aquaplaning of the driven wheels. This is experienced more likely at an FWD vehicle, where the driven wheels are exposed to a thicker water film compared to the rear wheels, where some water may have already been removed from the road by the front wheels.

In Figure 6 an acceleration manoeuvre with FWD vehicle A on the wet lane with 1.2 mm water level height is presented. The driver started to accelerate at 24 s with full throttle. Small spin-up events appear immediately and considerable wheel and vehicle speed differences can be observed at 25 s and 27 s. To better understand these two peaks, the traction coefficients for both front tyres were calculated and plotted based on the estimated engine torque. At 25 s, the traction coefficient dropped to 0.15, which indicates partial aquaplaning. At 27 s, the traction coefficient is below 0.05, which indicates total aquaplaning of the front right tyre. Although wheel spin-up with a low traction coefficient is a good indicator of aquaplaning, additional information is required to distinguish from similar effects at other low friction surfaces, such as ice- or snow-covered roads.

Next, the driver accelerates multiple times moderately with RWD vehicle B, releases the accelerator pedal, with two further repetitions on the wet lane with 1.1 mm water level height. The effect of the vehicle speed on the traction coefficients, derived during the emerging and pronounced wheel spin-up events, is outlined in Figure 7. The traction coefficient, which equals the coefficient of friction at the wheel spin-up events, declines with speed from about 0.55, for wet road conditions with partial aquaplaning, to about 0.05, for total aquaplaning conditions at the rear right tyre.

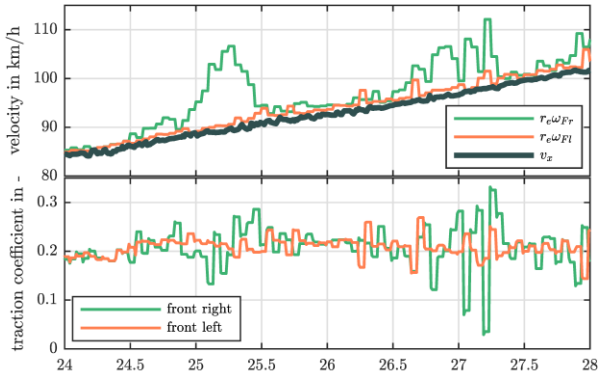

Figure 6

Wheel spin-up events and traction coefficient at FWD vehicle A; 1.2 mm water level height; medium worn summer tyres; nominal inflation pressure

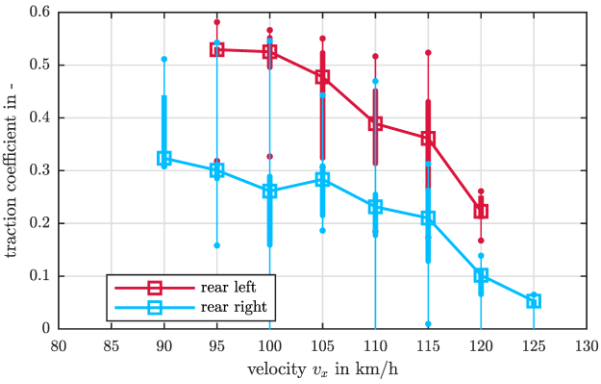

Figure 7

Traction coefficients from wheel spin-up events at RWD vehicle B; 1.1 mm water level height; very worn summer tyres; nominal inflation pressure

Combined wheel spin-up and wheel spin-down events appear when driving with RWD vehicle C at a constant speed above the total aquaplaning speed on the wet lane with 1.1 mm water level height, Figure 8. Immediately after entering the wet lane with 130 km/h, the front right wheels show a strong spin-down, while at the rear wheels only slight spin-up events can be observed. The driver held the steering wheel in centre position and applied about 40 % throttle to maintain velocity. After 13 seconds both rear wheels start to spin-up considerably, destabilizing the vehicle motion. An immediate, but initially very moderate growth of the yaw rate is noticeable. In reaction, the driver released the accelerator pedal and tried to stabilize the vehicle by steering, which was not successful, and the vehicle dangerously slided uncontrolled and turned around its vertical axis. After full braking on the dry road, the vehicle came to a complete stop some meters laterally

deviated from the straight wet lane. The addressed phenomena highlight a main difference between the behaviour of FWD and RWD vehicles at possible aquaplaning situations: a spin-up of the front wheels of an FWD vehicle, generally observed together with degraded acceleration potential and less responsiveness of the vehicle to steering input, typically indicates partial or total aquaplaning in general at lower speeds compared to an RWD vehicle, where the rear wheels face less water at the same speed. If the spin-down events of the front wheels of an RWD vehicle are ignored and speed is increased further, subsequent loss of stability can hardly be handled by the driver. Advanced autonomous driving motion control functions could offer solutions for handling such accidental situations in the future similarly as presented in [19].

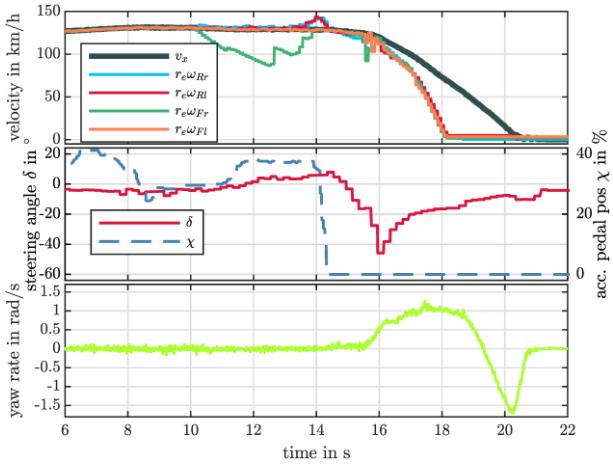

Figure 8

Loss of stability of RWD vehicle C at 130 km/h after wheel spin-up at the rear wheels; 1.1 mm water level height; medium worn summer tyres; nominal inflation pressure

3.3. Change of the Rolling Resistance

A tyre, rolling on a wet surface with a significant layer of water, will displace water from its contact patch depending on tread pattern (condition) and road surface, speed, water level height, etc. A water wedge develops at the leading edge and rolling resistance is increased, e.g. [7].

The estimation of the additional rolling resistance Δa_{res} from a wet road, which is derived from the difference of the nominal acceleration a_{nom} and the actually measured acceleration a_{meas} from the ESC sensor, including a given a_{offset},

$$a_{\mathrm{nom}} = \left(\sum_{i=1}^{4}\left(\frac{T_i}{r_{l,i}} - \frac{I_{w,i}\dot{\omega}_i}{r_{l,i}} - r_{w,i}\ F_{z,i}\right) - c_w v_x^2\right)/m \tag{2}$$

$$\Delta a_{\text{res}} = a_{\text{nom}} - a_{\text{meas}} + a_{\text{offset}}, \tag{3}$$

is a good indicator of the water level height, with vehicle mass m, aerodynamic drag coefficient c_w, vehicle velocity v_x, dry road rolling coefficient $r_{w,i}$, loaded radius $r_{l,i}$, wheel torque T_i and vertical tyre force $F_{z,i}$ of each wheel i.

Figure 9 shows the acceleration difference Δa_{res} for the transition from the dry asphalt lane to the wet lane with 108 km/h (constant) speed. The distinctive change of the rolling resistance indicator signal, which correlates to water level height and to speed, clearly marks the transition to the wet road where partial aquaplaning appears. The small delay of 0.3 s from signal processing of the water level sensor has not been removed.

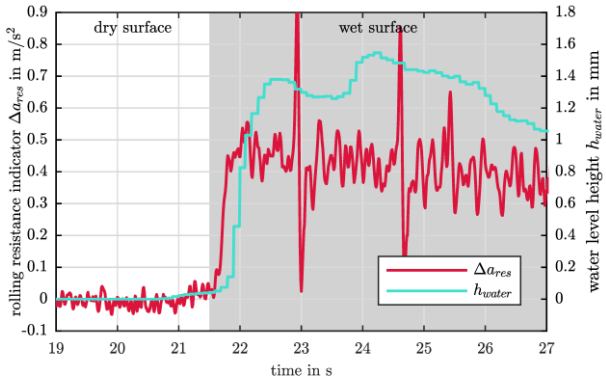

Figure 9

Rolling resistance indicator for transition with RWD vehicle B from dry asphalt to the wet lane with measured water level height; very worn summer tyres; nominal inflation pressure

In Figure 10(a) the influence of the water level height on the rolling resistance indicator for various manoeuvres is presented for RWD vehicle B with very worn summer tyres and nominal, i.e. low, inflation pressure. For all water level heights, the rolling resistance signal increases with speed. For (the three) lower water level heights, the rolling resistance indicators change in a similar way with speed. For 2 mm water level height, which represents a considerable amount of water on the road, both rolling resistance level and gradient increase with speed. For all water levels and speeds the minimum acceleration difference Δa_{res} is about 0.2 m/s².

Increased rolling resistance on the wet lane, with small water level heights as presented in this study, dominates changes in rolling resistance from tyre inflation pressure changes between low/medium/high on the dry lane. No clear influence of low/medium/high inflation pressures at RWD vehicle B on the rolling resistance indicator can be noticed in Figure 10(b), except for speeds close to total aquaplaning. The inflation pressure is 2.4/2.8 bar at the front and 2.7/3.3 bar at the rear tyres for medium/high nominal inflation pressure. The dry road rolling coefficient has not been adapted to the different tyre inflation pressures.

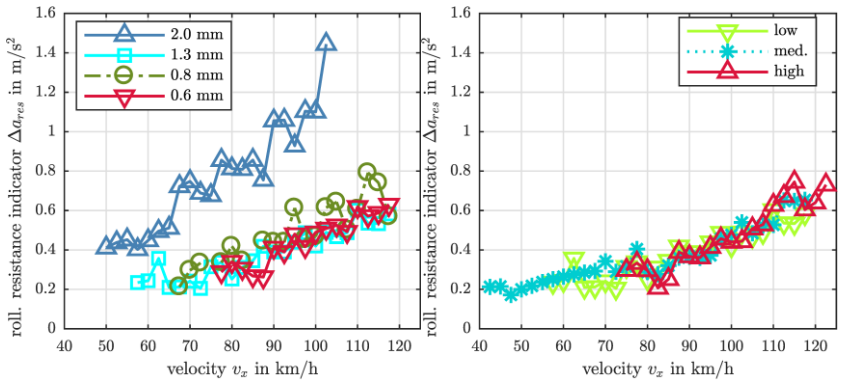

Figure 10

Rolling resistance indicator for RWD vehicle B; (a) for different speeds and water level heights; (b) for different speeds and tyre inflation pressures; very worn summer tyres; nominal inflation pressure

The influence of worn summer tyres and new winter tyres on the rolling resistance indicator is depicted in Figure 11 for two water level heights, 1.3 mm and 2 mm. The lines for the higher water level height are above the lines for the lower water level height. The lines for the worn summer tyres show a larger gradient and are above the lines for the new winter tyres, which may be attributed to the better lateral drainage capability of the winter tyres.

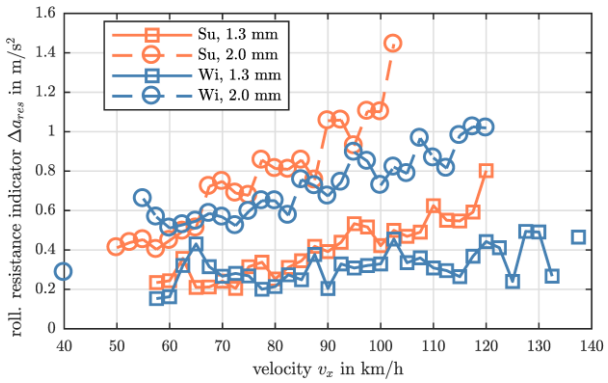

Figure 11

Rolling resistance indicator for RWD vehicle B with very worn summer tyres and new winter tyres; 1.3 mm and 2 mm water level heights; nominal inflation pressure

3.4. Change of the Slip Slope

Also, the gradient of the traction coefficient with respect to the longitudinal slip has been analysed. It has been reported that the measured slip slope changes on low friction surfaces, [20], so a change of slip slope might be expected at aquaplaning

conditions as well, which will be addressed now in more detail. Although basic tyre modelling theory gives no reason to expect a dependency of the slip slope from the friction coefficient, [21], the additional intermediate layer between tyre and road, such as snow or ice, and other possible effects are proposed as possible reasons for the observations, e.g. [22]. At partial aquaplaning, the wet contact area will not contribute to the horizontal shear stresses, so the reduction of the contact patch length is the main cause for the lower slip slopes. The reduction of the contact patch length, depending on speed and tyre inflation pressure, is characterized in [6], [9].

Figure 12 includes the calculated traction coefficients and longitudinal slips on dry and wet asphalt from Figure 9. The normalized slip slopes $\bar{C}_{sx}$ for the dry and the wet lane are included and reveal that the measured slip slope considerably decreased at partial aquaplaning.

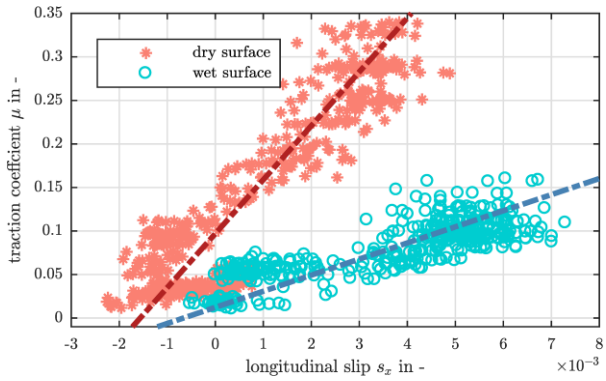

Figure 12

Traction coefficient and longitudinal slip data points with fitted slip slope for the dry and the wet asphalt lane corresponding to Figure 9

Figure 13(a) shows the slip slope change of the driven wheels of RWD vehicle B as a function of speed for the worn summer tyres with nominal inflation pressure. The resulting curves clearly outline the expected decrease of the derived slip slopes for higher speeds with increasing partial aquaplaning. Slip slopes for the left hand-side are higher than for the right-hand side as one would expect from the discussion in context with Figure 4(b). The slip slope of these tyres and inflation pressure on dry asphalt is approximately 100. Interestingly, the change of the water level height from 0.6 mm to 2.0 mm in four steps does not show a clear influence on the slip slope curves. A possible explanation is that the residual water film at the rear wheels, which the front tyres did not displace, does not change in the amount as for the front tyres. Nevertheless, the observed difference for the left and right tyres from the inhomogeneity of conditions at both sides remains, and both effects may contribute in some way to the presented characteristics.

In Figure 13(b) the tyre inflation pressure is varied for the worn summer tyres at the RWD vehicle B and a nominal water layer height of 1.3 mm.

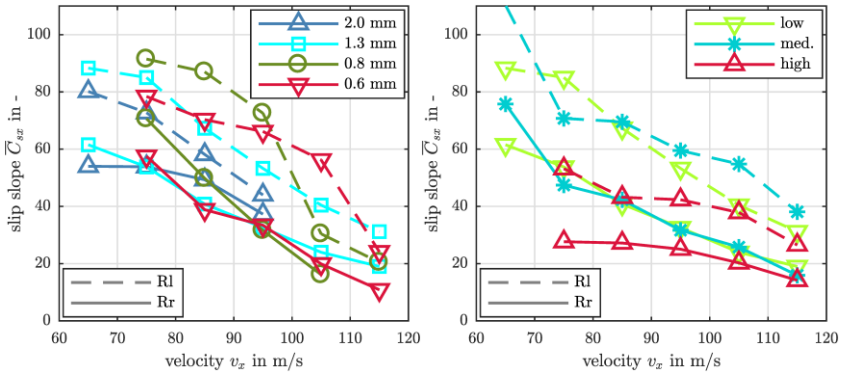

Figure 13

Slip slope at rear tyres (very worn summer tyres, nominal inflation pressure) of RWD vehicle B (a) for different speeds and water level heights; (b) for different speeds and inflation pressures; 1.3 mm water level height

All slip slope curves have a negative gradient at partial aquaplaning and again a difference between left and right wheels appears. While the slip slope curves for the low and medium inflation pressure show a similar level, the level for the high inflation pressure is clearly lower. For low speeds between 60 to 80 km/h only few valid data points were available, which leaves some uncertainties in this range.

In contrast to summer tyres, tests with new winter tyres on RWD vehicle B show that over the whole considered speed range from 60 to 130 km/h, the estimated slip slope remains at low levels with no significant gradient, Figure 14. Obviously, the winter tyres do not experience any significant partial aquaplaning for both water level heights and all speeds.

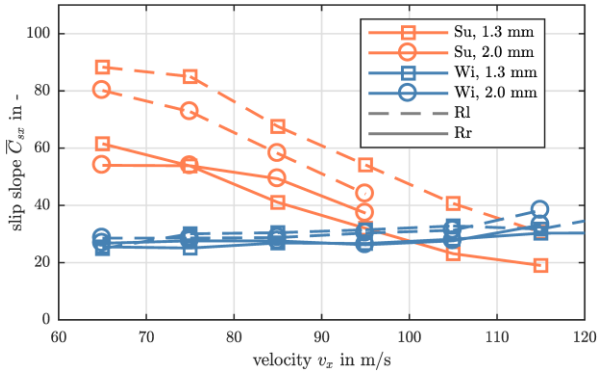

Figure 14

Slip slope at rear tyres of RWD vehicle with medium worn summer tyres and new winter tyres; 1.3 mm and 2 mm water level heights; nominal inflation pressure

3.5. Change of the Tie Rod Forces

An indication for total aquaplaning at the front tyres is a light steering torque experienced by the driver. In this case, almost no lateral tyre forces are developed and also no aligning moments appear. Experience from several manoeuvres during this study shows, that even for small required corrections to keep the intended path, drivers tend to increase the steering angle as long they do not see the expected vehicle reaction (yaw rate). This is in particular critical, if, for example, full aquaplaning ends at one front tire and lateral forces are developed suddenly, which may result in a spinning vehicle.

Tie rod forces, which include components of lateral/longitudinal/vertical tyre forces and aligning moment, depend on coefficient of friction between tyres and road. Therefore, they have been suggested to estimate the friction coefficient, e.g. in [23] and [24], but could be relevant to detect effects of partial and total aquaplaning as well.

Modelling and reliably estimating the aligning moment in the remaining contact patch at partial aquaplaning condition, including areas of adhesion and sliding, appears to have little prospect of success due to many influences, which are difficult to quantify themselves. CFD and FEM simulation [25] will help in this respect and support better understanding, but is beyond the scope of this publication and will not suit for real time aquaplaning detection methods.

Instead, a comparison of calculated tie rod forces, on the assumed dry lane, with measured forces, on the actual wet lane, is proposed, that could indicate partial aquaplaning, similar to the rolling resistance indicator in Chapter 3.3. Based on a quasi-static vehicle model, vertical tyre forces are determined from vehicle mass, geometry and measured longitudinal and lateral accelerations. The front lateral tyre forces are calculated from a simple 2-wheel vehicle model and distributed between left and right proportional to the vertical tyre forces. Basic parameters for the front suspension geometry like, e.g. individual tyre steering angles, tie rod lever arms, kinematic trails, etc., are derived from MBD simulations and are included as polynomials over steering wheel angle. There results the tie rod forces $F_{tr,i} = F_{tr,i}(\delta_i, F_{x,i}, F_{y,i}, F_{z,i})$ for each front wheel i.

A (almost) constant speed, without longitudinal tyre forces at the front wheels, acceleration manoeuvre with longitudinal traction forces, and a constant speed slalom manoeuvre with AWD vehicle D running over the aquaplaning basin will be discussed subsequently.

For the constant speed, straight-line driving manoeuvre in Figure 15(a), typical spin-down aquaplaning events appear at the front right wheel. The right wheels were running in the aquaplaning basin with a water level height of about 2 mm, whereas the left wheels were running on damp asphalt. Both front wheels can be considered free rolling since no traction torque was distributed to the front axle.

Total aquaplaning causes a significant change of the measured tie rod forces, which change to a much higher level in comparison to the calculated nominal values. Obviously, the changing of conditions in the tyre contact patch, such as contact length, friction coefficient, pressure distribution, due to partial or total aquaplaning condition will lead to changes in the wheel force balance and therefore in the steering torque, felt by the driver or recorded by tie rod force transducers. Even during very short spin-downs, e.g. at 12.6 s and 18.7 s, measured tie rod forces at the front right wheel differ significantly from the calculated forces. At the end of the spin-downs, the measured tie rod forces immediately decrease to the level of the calculated forces. The measured left tie rod force is similar to the calculated forces, but shows small differences during larger spin-downs of the right wheel.

In Figure 15(b) a rather extreme manoeuvre is presented with repetitions of accelerating with 1-1.5 m/s² in the aquaplaning basin with 7 mm water level height, similar to filled wheel ruts on a road. The entry speed at 17 s is already close to the aquaplaning speed and a minor decrease of the wheel speed occurs at the front left wheel immediately. In contrast, to the spin-downs from total aquaplaning at the previous manoeuvre, Figure 15(a), a small amount of traction torque was distributed to the front wheels at the beginning of the acceleration period at 17 s, which prevented the development of a large spin-down. With increased speed and acceleration, the left wheel speed increases again and even shows a short spin-up event at 19 s. Despite aquaplaning causes only small deviations of the wheel speeds here, the corresponding tie rod forces change dramatically. At the end of the second acceleration period between 22.8 s to 24.5 s, the front left wheel shows a large spin-up followed by a short spin-down at 25 s. The measured tie rod forces again differ significantly from their nominal values and increase in both cases for spin-up and spin-down.

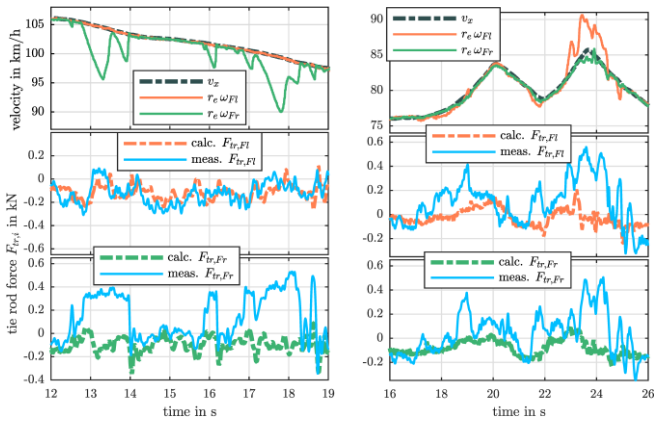

Figure 15

(a) Tie rod force indicator of AWD vehicle D for a constant speed, straight-line driving manoeuvre; medium worn summer tyres; nominal inflation pressure; 2 mm water level height; (b) Tie rod force indicator of AWD vehicle D for an acceleration, straight-line driving manoeuvre; medium worn summer tyres; nominal inflation pressure; 7 mm water level height

The final manoeuvre, Figure 16, is a moderate slalom at almost constant speed and lateral accelerations of 1-2 m/s². Wheel speeds show a series of short spin-down events at both tyres. A mismatch between steering angle (driver input) and lateral acceleration (vehicle reaction) becomes obvious when total aquaplaning at both front tyres occurs at 23.2 s, 25.4 s and from 27.3 s to 27.7 s.

Although changes of tie rod forces can give a good indication of aquaplaning at a tyre, their measurement requires additional sensors that are not common in production cars. An alternative is the utilization of an available total steering rack force, which can give limited information on a change in individual tie rod forces. In case of aquaplaning at both front wheels, the steering rack force does not change, but in case of one-sided aquaplaning, a clear difference to nominal values can be detected. Alternatively, in case of full aquaplaning at both wheels, steering angle, lateral acceleration and yaw rate in combination with the steering rack force may serve as a good indicator instead.

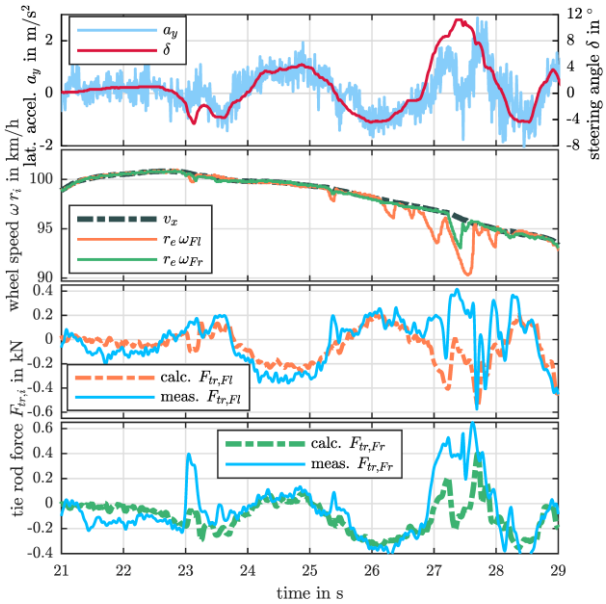

Figure 16

Tie rod force indicator of AWD vehicle D for a constant speed slalom manoeuvre; medium worn summer tyres; nominal inflation pressure; 7 mm water level height

Conclusions

Early warning, avoidance or reduction of risk of aquaplaning requires a reliable detection and interpretation of typical aquaplaning effects at the tyres. The aim of this paper is to show different manifestations of aquaplaning based on measurements with standard sensors. In particular, wheel spin-up and wheel spin-down, change of rolling resistance, tyre slip slope, and tie rod force have been

considered manifestations of partial or total aquaplaning. Based on this, a mathematical evaluation of these effects and their combination could be realized and an aquaplaning detector/predictor developed. An example thereof has already been introduced in [26].

Although the addressed manifestations indicate aquaplaning conditions in a quite obvious manner, a lot of influences need to be accounted for a reliable detection method of partial aquaplaning and for separation from other low friction surfaces. Driveline configuration, type, wear and inflation pressure of the tyre(s), water level height next to chosen speed and performed manoeuvre significantly affect these manifestations. A selection of results is presented here, both to encourage the development of a possible detection method and to point out the difficulties involved. A focus has been set to road conditions with low water level heights between 0.6 and 2.0 mm that the driver may not identify as critical and therefore end up in more dangerous aquaplaning situations at higher velocities. While scientific literature on aquaplaning is most frequently related to tyre development, aquaplaning is addressed here from a vehicle dynamics application point of view.

For the driver it was easier to detect (partial) aquaplaning with the FWD vehicle due to wheel spin-up events and increased rolling resistance at the front wheels, affecting acceleration and noise, the sensed changes in steering torque and lateral responsiveness of the vehicle. The characteristic spin-down effect at the front wheels is especially useful to be sensed and evaluated at RWD vehicles, as (partial) aquaplaning might be noticed only at higher speeds, as rear wheels run in the track of the front wheels and need to displace less water. The AWD vehicle showed characteristics of both FWD and RWD vehicles. Consequently, a detection method should include knowledge on the drive torque distribution control.

As a good indicator of a critical water level height at a given speed is the increased rolling resistance. Another good indicator of partial aquaplaning is the drop of the measured slip slope due to the reduced contact length of the tyre. However, sufficient amount of longitudinal force/slip excitation is required and additional effects/sensors need to be evaluated to separate wet from other low friction road surfaces. As an example for an additional sensor, tie rod forces, or alternatively the steering rack force, give similar indication of possible aquaplaning that also the driver could feel next to degraded responsiveness of the vehicle.

On-board information on tyre type, wear condition from mileage and average workload, and inflation pressure are essential for robust prediction of aquaplaning conditions. Further benefits are to be expected from other on-board sensors to map or estimate water level and/or vehicle states, next to sensor systems for automated driving that are able to sense road conditions ahead of the vehicle.

Acknowledgement

The measurement was carried out for R&D purposes at the ZalaZONE Automotive Proving Ground within the framework of scientific cooperation.

The research reported in this paper and carried out at the Budapest University of Technology and Economics has been supported by the National Research Development and Innovation Fund (TKP2020 Institution Excellence Subprogram, Grant No. BME-IE-MIFM) based on the charter of bolster issued by the National Research Development and Innovation Office under the auspices of the Ministry for Innovation and Technology.

In addition, the research was supported by the Ministry of Innovation and Technology NRDI Office within the framework of the Autonomous Systems National Laboratory Program

References

[1] S. Baskara, Sudesh and Yaacob, Haryati and Hainin, Mohd Rosli and Hassan "Accident due to pavement condition – A review," *J. Teknol.*, Vol. 78, No. July, 2016, doi: 10.11113/jt.v78.9494

[2] T. F. Fwa, K. Anupam, and G. P. Ong, "Relative effectiveness of grooves in tire and pavement for reducing vehicle hydroplaning risk" *Transp. Res. Rec.*, No. 2155, pp. 73-81, 2010, doi: 10.3141/2155-08

[3] F. Spitzhüttl, F. Goizet, T. Unger, and F. Biesse, "The real impact of full hydroplaning on driving safety" *Accid. Anal. Prev.*, Vol. 138, No. September 2019, p. 105458, 2020, doi: 10.1016/j.aap.2020.105458

[4] S. Das, A. Dutta, K. Dey, M. Jalayer, and A. Mudgal, "Transportation Research Interdisciplinary Perspectives Vehicle involvements in hydroplaning crashes : Applying interpretable machine learning" *Transp. Res. Interdiscip. Perspect.*, Vol. 6, p. 100176, 2020, doi: 10.1016/j.trip.2020.100176

[5] J. M. Mounce and R. Bartoskewitz, "Hydroplaning and Roadway Tort Liability" *Transp. Res. Rec.*, No. 1401, pp. 117-124, 1993

[6] W. B. Horne and R. C. Dreher, "Phenomena of pneumatic tire hydroplaning" no. November 1963, 1963, [Online] Available: https://ntrs.nasa.gov/search.jsp?R=19690028143

[7] W. Gengenbach, "The Effect of Wet Pavement on the Performance of Automobile Tires" Buffalo, New York, 1967

[8] B. J. Allbert, "Tires and hydroplaning" *SAE Tech. Pap.*, 1968, doi: 10.4271/680140

[9] A. J. Niskanen and A. J. Tuononen, "Three 3-axis accelerometers fixed inside the tyre for studying contact patch deformations in wet conditions," *Veh. Syst. Dyn.* Vol. 52, No. SUPPL. 1, pp. 287-298, 2014, doi: 10.1080/00423114.2014.898777

[10] A. Tuononen and L. Hartikainen, "Optical position detection sensor to measure tyre carcass deflections in aquaplaning" *Int. J. Veh. Syst. Model.*

Test., Vol. 3, No. 3, pp. 189-197, 2008, doi: 10.1504/IJVSMT.2008.023837

[11] R. C. Dreher and W. B. Horne, "Ground-Run Tests with a Bogie Landing Gear in Water and Slush" 1966

[12] A. J. Stocker, And, J. T. Dotson, And, and D. L. Ivey, "Automobile tire hydroplaning - a study of wheel spin-down and other variables" *Texas Transp. Inst. Res. Rep. Number 147-3F*, no. August, 1974

[13] W. B. Horne and U. T. Joyner, "Pneumatic tire hydroplaning and some effects on vehicle performance" *SAE Tech. Pap.*, 1965, doi: 10.4271/650145

[14] A. J. Stocker and J. M. Lewis, "Variables associated with automobile tire hydroplaning" no. September, 1972

[15] S. Mahadevan and S. Taheri, "Review of vehicle hydroplaning and tire-pavement interactions" 2017

[16] "MARWIS: Mobile collection of weather data in real time," [Online] Available: https://lufft-marwis.de/en/

[17] Z. Szalay, Z. Hamar and Á. Nyerges, "Novel design concept for an automotive proving ground supporting multilevel CAV development" *International Journal of Vehicle Design*, Vol. 80, No. 1, 2019

[18] J. E. Martinez, J. M. Lewis, and A. J. Stocker, "A study of variables associated with wheel spin-down and hydroplaning" Proc. of 51st Annual Meeting of the Highway Research Board, 1972

[19] Á. Bárdos, Á. Domina, V. Tihanyi, Z. Szalay and L. Palkovics, "Implementation and experimental evaluation of a MIMO drifting controller on a test vehicle" 2020 IEEE Intelligent Vehicles Symposium (IV), 2020, pp. 1472-1478, doi: 10.1109/IV47402.2020.9304820

[20] T. Dieckmann, "Erkenntnisse aus der bisherigen Entwicklung des schlupfbasierten Kraftschlußpotential-Meßsystems" Hannover, Deutschland, 1993

[21] H. B. Pacejka, *Tire and Vehicle Dynamics* Third edit. Butterworth-Heinemann, 2012

[22] C. Deur, Joško ; Ivanović, Vladimir ; Pavković, Danijel ; Asgari, Jahan ; Hrovat, Davor ; Troulis, Markos ; Miano, "On low-slip tire friction behavior and modeling for different road conditions" in *Proceedings of 19th IAVSD Symposium - Poster Papers*, 2005, pp. 1-10

[23] Y.-H. J. Hsu and J. C. Gerdes, "A Feel for the Road: A Method to Estimate Tire Parameters Using Steering Torque" 2006

[24] M. J. Matilainen and A. J. Tuononen, "Tire friction potential estimation from measured tie rod forces" *IEEE Intell. Veh. Symp. Proc.*, no. Iv, pp. 320-325, 2011, doi: 10.1109/IVS.2011.5940528

[25] H. C. Jung, M. D. Jung, K. M. Jeong, and K. Lee, “Verification of Tire Hydroplaning Phenomenon Using Coupled FSI Simulation by CFD and FEM” *Open J. Appl. Sci.*, Vol. 10, No. 07, pp. 417-431, 2020, doi: 10.4236/ojapps.2020.107029

[26] A. Fichtinger, J. Edelmann, M. Plöchl and M. Höll, "Aquaplaning Detection Using Effect-Based Methods: An Approach Based on a Minimal Set of Sensors, Electronic Stability Control, and Drive Torques" IEEE Vehicular Technology Magazine, Vol. 16, No. 3, pp. 20-28, Sept. 2021, doi: 10.1109/MVT.2021.3085536